

*Land use and land cover changes in  
Doume Communal Forest in eastern  
Cameroon: implications for conservation  
and sustainable management*

**Jules Christian Zekeng, Reuben Sebego,  
Wanda N. Mphinyane, Morati Mpalo,  
Dileswar Nayak, Jean Louis Fobane, Jean  
Michel Onana, et al.**

**Modeling Earth Systems and  
Environment**

ISSN 2363-6203

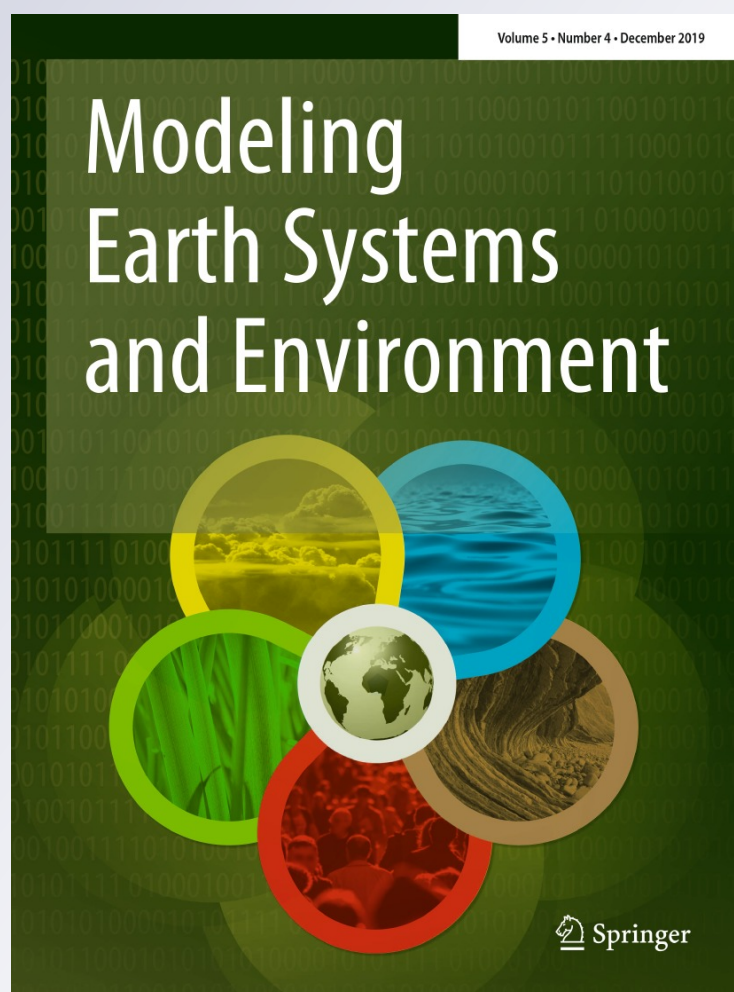
Volume 5

Number 4

Model. Earth Syst. Environ. (2019)

5:1801-1814

DOI 10.1007/s40808-019-00637-4



**Your article is protected by copyright and all rights are held exclusively by Springer Nature Switzerland AG. This e-offprint is for personal use only and shall not be self-archived in electronic repositories. If you wish to self-archive your article, please use the accepted manuscript version for posting on your own website. You may further deposit the accepted manuscript version in any repository, provided it is only made publicly available 12 months after official publication or later and provided acknowledgement is given to the original source of publication and a link is inserted to the published article on Springer's website. The link must be accompanied by the following text: "The final publication is available at [link.springer.com](https://link.springer.com)".**



# Land use and land cover changes in Doume Communal Forest in eastern Cameroon: implications for conservation and sustainable management

Jules Christian Zekeng<sup>1,2</sup> · Reuben Sebego<sup>2</sup> · Wanda N. Mphinyane<sup>2</sup> · Morati Mpalo<sup>2</sup> · Dileswar Nayak<sup>3</sup> · Jean Louis Fobane<sup>4</sup> · Jean Michel Onana<sup>1</sup> · Forbi Preasious Funwi<sup>1</sup> · Marguerite Marie Abada Mbolo<sup>1</sup>

Received: 21 May 2019 / Accepted: 21 August 2019 / Published online: 6 September 2019  
 © Springer Nature Switzerland AG 2019

## Abstract

Large-scale identification of land use and land cover change in a tropical forest is a challenge to landscape designers and forest ecologists. Here, Landsat images acquired during the years 2000, 2009, and 2018 were used to assess the spatial-dynamics of land use and land cover (LULC) during the last two decades (2000–2018). A classification system composed of six classes—dense forest with (high tree density and low tree density), swampy *Raphia* forest, swampy flooded forest and savanna were designed as LULC for this study. A maximum likelihood classification was used to classify Landsat images into thematic areas. Elsewhere, Landsat-based LULC mapping, post classification at the per-pixel scales and self-knowledge on the land cover change processes were combined to analyze LULC change, forest loss and change trajectories in Doume Communal Forest in eastern Cameroon. The results show that half of the study area changed in 2000–2009 and that the different types of LULC changes increased and involved more diverse and characteristic trajectories in 2009–2018 compared to 2000–2009. Degradation to a dense forest with low tree density and swampy *Raphia* forest was dominant, and the forest was mostly lost due to trajectories that involved conversion to agroforestry systems (10%), and a lesser extent due to trajectories that involved deforestation to grasslands (7%). The trajectory analyses did thus contribute to a more comprehensive analysis of LULC change and the drivers of forest loss and, therefore, is essential to improve the sustainable management and support spatial planning of the forest.

**Keywords** Geographic information systems · Land use/land cover changes · Land management · Multi-temporal Landsat imagery · Remote sensing · Tropical rainforest · Cameroon

## Introduction

Land use and land cover (LULC) comprises two separate terminologies which are often used interchangeably (Dimiyati et al. 1996). Land cover refers to the physical characteristics of the earth's surface, captured because the distribution of vegetation, water, soil and other physical features of the land, including those created by anthropogenic activities. Land use, however, refers to the way land is used by humans including all infrastructure, usually highlighting the functional role of land for their economic activities (Rawat and Kumar 2015). The LULC pattern of ecosystems is an outcome of natural and socio-economic factors and their spatial–temporal utilization. Information on LULC and prospects for his or her optimum use is crucial for the choice, planning, and implementation of land use schemes to satisfy the increasing demands for basic human needs and welfare.

**Electronic supplementary material** The online version of this article (<https://doi.org/10.1007/s40808-019-00637-4>) contains supplementary material, which is available to authorized users.

✉ Jules Christian Zekeng  
[juleschris006@yahoo.fr](mailto:juleschris006@yahoo.fr)

<sup>1</sup> Department of Plant Biology, Faculty of Science, University of Yaounde I, P.O. Box 812, Yaoundé, Cameroon

<sup>2</sup> Department of Environmental Science, Faculty of Science, University of Botswana, Private Bag UB 0704, Gaborone, Botswana

<sup>3</sup> Department of Natural Resource Management ASPEE Colleges of Horticulture and Forestry, Navsari Agricultural University, Navsari 396450, Gujarat, India

<sup>4</sup> Department of Biology, Higher Teachers' Training College, University of Yaounde I, P.O. Box 47, Yaoundé, Cameroon

This information also assists in monitoring the dynamics of land use resulting from the changing demands of the increasing populations.

Studies on LULC (e.g. Lambin et al. 2001; Geist and Lambin 2002; Kibret et al. 2016; Gidey et al. 2017; Kindu et al. 2018; Momo Solefack et al. 2018) show that socio-economic and biophysical variables act as the driving forces of land use changes. Miheretu and Yimer (2017) subdivided these drivers into two groups: proximate causes and underlying causes. Proximate causes are the activities and actions that have an affect on land use, e.g. wood extraction or road construction. Underlying causes are the elemental forces that underpin the proximate causes, together with demographic, economic, technological, institutional and cultural factors (Geist and Lambin 2002), that represent the biggest driver of biodiversity loss and climate change (Bellard et al. 2012; Zari 2014; Wu et al. 2017). Due to these global drivers, LULC change is present in all environments across the globe (Lambin et al. 2001; Geist and Lambin 2002).

Each year large surfaces of tropical forests are profoundly transformed by anthropogenic activities (Le Toan et al. 2011; Harris et al. 2012; Le Quéré et al. 2013; Malhi et al. 2014; Le Quéré et al. 2016). Due to the huge negative impact of forest loss on global climate change and ecosystem services, tropical deforestation is considered as the most paradigmatic example of LULC change (Foley et al. 2005). During the last two decades, 80% of new agricultural land across the world came from the conversion of tropical forest (Gibbs et al. 2010; Pendrill and Persson 2017) meaning that about one-third of the global land surface is classified under this land use (Ellis et al. 2010; Sebastian et al. 2015).

The forests of Cameroon, with around 22.5 million ha of forest cover, or 48% of the national territory, represents the second largest tropical forest area in Congo Basin after those of the Democratic Republic of Congo (De Wasseige et al. 2009). According to the FAO, the annual average deforestation rate in Cameroon for the 1980–1995 period was 0.6% or a loss of close to 2 million ha (WRI, UNEP, UNDP and World Bank 1998). During 1999–2000, however, the deforestation rate was close to 0.9%, and reached 1% between 2000 and 2005 (FAO 2006). Between 1990 and 2010, it is estimated that Cameroon lost 4400 ha (18.1%) (FAO 2011). This fast deforestation rate of destructing ecosystems is a major threat to global biodiversity (Myers 1988; Sangermano et al. 2012; Marchese 2015). It also compromises the future of many indigenous people as well as the future of local populations (Lewis et al. 2009; Smail and Lewis 2009). Understanding LULC change and its underlying factors is important for biodiversity conservation and climate change mitigation policies.

LULC change can contribute to climate change through changes in the global carbon cycle (Davies-Barnard et al. 2015). Such impacts underpin several global initiatives

that Cameroon has subscribed to, such as REDD+ and the Nagoya protocol of the Biological Diversity agreement, which seeks to reduce LULC change patterns and their impacts on biodiversity (CBD 2005). However, the success of such initiatives relies in part on sound scientific information on LULC change levels in tropical regions and their evolution over time, but quantitative data on LULC change are generally incomplete and unreliable (Ramankutty et al. 2007; Grainger 2008; Grainger 2010). Even though LULC change has attracted much attention over the last three decades, for lower-income countries, understanding their process and structure over the space and time remains one of the major challenging activities (Ghilardi et al. 2016).

Several studies used remote sensing and geographic information system (GIS) tools to obtain accurate and timely spatial data of land use and land cover, as well as information on the changes in a study area (e.g. Gidey et al. 2017; Momo Solefack et al. 2018). Remote sensing images can effectively record the current status of land use and provide an excellent source of data, from which updated LULC information and changes can be extracted, efficiently analyzed through certain means (Pradhan et al. 2008; Singh et al. 2017). Therefore, remote sensing is widely used in the detection and monitoring of land use at different intervals and scales (Lu et al. 2012a; Basnet and Vodacek 2015; Momo Solefack et al. 2018) while GIS provides a flexible environment for collecting, storing, displaying and analyzing digital data necessary for change detection.

While these tools are of unparalleled importance for forest sustainable management and monitoring, it is also true that they are not frequently used by forest managers both at the national and local level. This study focuses on the Doume Communal Forest (DCF) situated in eastern Cameroon and belonging to the guineo-Congolese domain (Letouzey 1985). The forest is crucial for both national development and the livelihoods of about 22,763 local inhabitants (Anonymous 2015). This forest is subject to intense pressure due to rapid population growth, logging and hunting activities that exert a diverse ecological impact on the forest ecosystems. Therefore, to address the challenges of global change, vulnerability, resilience and adaptive capacity of the forest ecosystem and improve the management and monitoring of natural resources, timely, accurate and up to date information of LULC change and trajectories are required.

This study aims to analyze the land cover changes and trajectories that have occurred in Doume Communal Forest over the past two decades (2000–2018) using the integration of remote sensing and GIS applications. We address the question: what are the dynamics and the trajectories of LULC in the DCF for the three periods of 2000–2009, 2009–2018, and 2000–2018? Considering the process of Doume Communal Forest classification started in 2008 and assuming that its management follows the principles



of sustainable management, it is expected that the dynamics and change trajectories of LULC for the second decade 2009–2018 would be lower than for the first decade 2000–2009.

## Materials and methods

### Study area

The study was conducted within the semi-deciduous forest, Doume Communal Forest (DCF) in eastern Cameroon (4°31'0"S and 13°47'5"W). The forest is managed by the Doume municipality and cover an area of 45,359 ha divided into two blocks (25,810 ha for block 1 and 19,549 ha for block 2). The first block is located between 4°16'N, 4°32'N, 13°16'E, and 13°32'E and shares boundaries with the Doumantang Communal and Bayong community forests. The second block is located between 4°8'N, 4°16'N, 13°12'E and 13°32'E and shares boundaries with the Angossas Communal forest (Fig. 1). The vegetation belong to the guineo-Congolese domain and classified as Sterculiaceae and Ulmaceae forest (Letouzey 1985).

The DCF lies within the geological bedrock. Some areas characterized by the presence of migmatic gneisses and anatectic granites belonging to the Precambrian base complex dated between 2.5 and 1.8 billion years (Nougier 1979 cit.

Anonymous 2015). The soils are derived from the alteration of metamorphic source rocks widely dominate. The DCF is covered mostly by ferrallitic red soils, loose and permeable, with little humus which can be several meters thick and the minerals are completely hydrolyzed with the removal of bases and silica. These soils are poor in nutrients, acids and fragile. In the shallows, the soils are hydromorphic to gley (Anonymous 2015). Relatively uniform, the relief of the forest can be described as slightly uneven. It presents a succession of low hills with generally gentle slopes interspersed with small well-marked streams, or swampy depressions (several hundred meters) without a distinct watercourse. Steep slopes can be observed but they remain much localized on the edge of lowlands or rivers, and their difference in level seldom exceeds 20–30 m. The altitude varies from 605 to 760 m, with some particularly marked summits, culminating at less than 700 m of altitude (Anonymous 2015).

The DCF is localized in locality with an Equatorial Guinean climate type characterized by (1) an annual rainfall included between 1300 and 1800 mm with 02 rainy seasons interspersed by two dry seasons and distributed; (2) the annual average temperature is 25 °C with an amplitude of 2.4 °C. It varies between 25 and 30 °C from March to November. Whereas, from December to February, the hottest months, the temperature can reach 35 °C; (3) the seasonal cycle is mainly governed by the annual movements of the intertropical front, between the

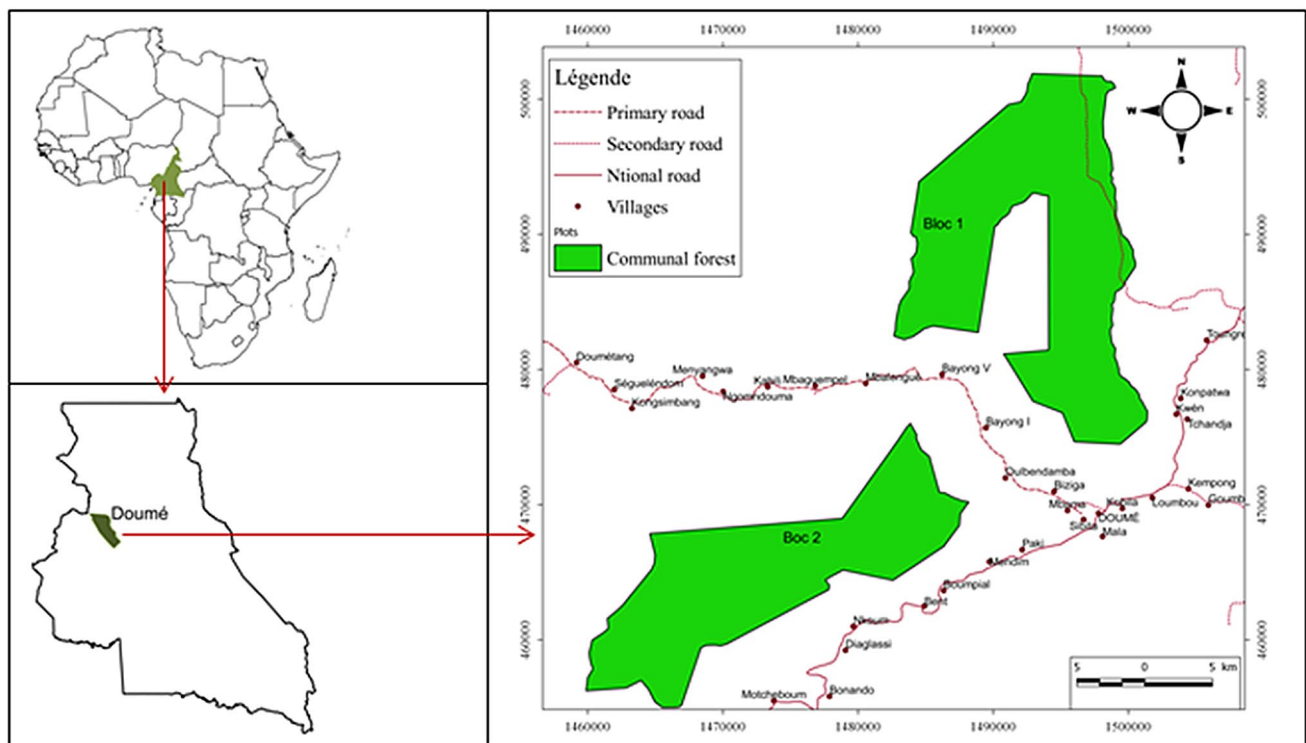


**Fig. 1** Map and localization of the Doume Communal Forest, showing the two blocks (FC DOUME block 1 and 2) of Doume Communal Forest

convergence zones of the southern trade winds and the northern trade winds. On the Nyong Basin these displacements result in dry winds from December to February, relatively wet winds from March to July, wet from August to October and relatively dry in November.

## Data collection and research methods

This study used remote sensing, GIS techniques and field data to classify and map the current and historic LULC. The overview of the research design, including all remote sensing and GIS techniques used, is summarized by the flow chart (Fig. 2).

### Satellite images

We obtained free cloud cover Landsat 7 Enhance Thematic Mapper Plus (ETM+) images for the years 2000 and 2009, and Landsat 8 Operational Land Imager and Thermal Infrared Sensor (OLI/TIRS) 8 images for the year 2018. The images scenes were designated by path 184/row 057 and acquired from <https://earthexplorer.usgs.gov>, the United State Geological Survey (USGS) Landsat archive. Furthermore, we obtained “Satellite Pour l’Observation de la Terre” (SPOT) 7 images for the study area from Airbus Defence and Space, which were available through the project “Observation Spatiale des Forêts d’Afrique Centrale et de l’Ouest” (OSFACO, <http://www.osfaco.org>). However, these SPOT images did not cover the entire study area and were, therefore, only used to obtain additional reference data to validate further classification.

### Field data collection and land use/land cover classification

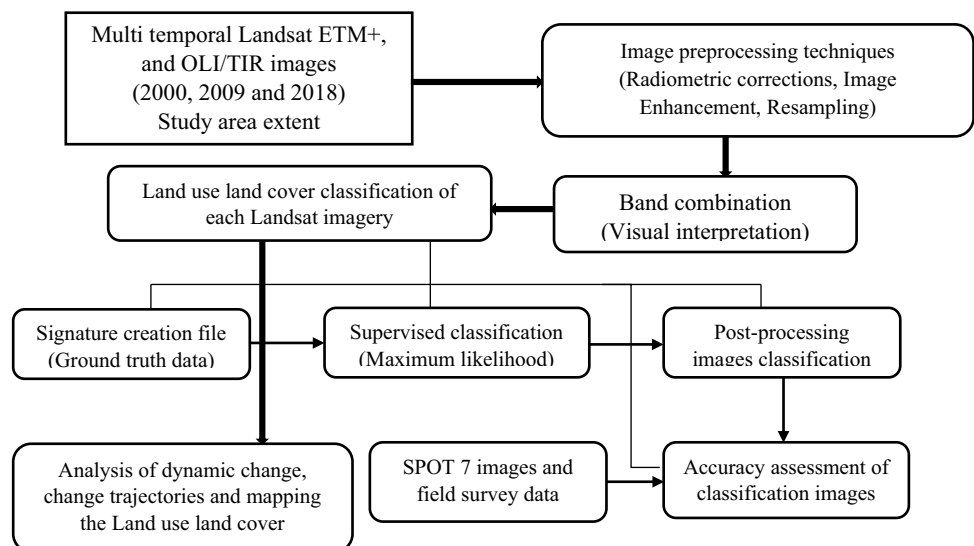
To classify the landscape into different LULC classes, we used the classification scheme developed by the Doume Forest Council, derived from earlier field observations in the landscape. These included the following LULC classes: swampy *Raphia* forest (RphSF), swampy flooded forest (SwFF), grasslands (GrLD), dense forest with low tree density (DFTLD), dense forest with high tree density (DFHTD), agroforestry systems land (AgrL).

We performed field surveys to categorize the landscape into the abovementioned LULC classes, for two applications: as training samples for landscape classification (see “[Supervised classification](#)”), and as reference data for accuracy assessment (see “[Post classification](#)”). Field surveys were conducted from June–August 2018 and four hundred ground truthing data were collected using a Garmin 62S GPS for all LULC type. The great challenge in tropical dense forests is the accessibility of remote areas of the forest interior. Therefore, the obtained SPOT 7 images over the study area were used to collect fifty sampling points in the remote areas where the field team could not access. To collect the reference data for 2000–2009 period, Google Earth Pro was used. We additionally described the area using the management plan of the Doume Communal Forest where extensive field inventory was done to describe the LULC classes.

### Image pre-processing

We took three steps for the pre-processing of the Landsat images. First, we had to make sure that information from all bands to be used (seven first bands; Table S1) had the same spatial resolution, so that their information could be combined. Furthermore, as all the images had previously been related to the Universal Transverse Mercator (UTM)

**Fig. 2** Flow chart of the research methodology



coordinate system 33 N, and that their geometric accuracy met our research requirement, there was, therefore, no need for any further geometric correction. Second, as the Landsat 7 ETM+ and Landsat 8 OLI/TIRS, did not have the same spatial resolution, there was a need to improve the Landsat 7 ETM+ with 30 m  $\times$  30 m so that it had the same spatial resolution of Landsat 8 OLI/TIRS. For that, we used the image enhancement Ehlers fusion resolution merge technic (Ehlers 2004), which has the aptitude for creating multispectral images of higher spatial resolution while preserving the spectral characteristics of the lower resolution multispectral images (Lu et al. 2011; Chitade and Katiyar 2012). To avoid the change of digital numbers and keep the images at the same pixel size of 30 m by 30 m, during image-to-image registration, the nearest neighbour resampling algorithm was used to resample (Li et al. 2011) the TM+ and OLI images. Therefore, the spatial resolution of all products was improved from 30 m  $\times$  30 m into 15 m  $\times$  15 m. Third, for each year's images, we combined the first seven bands into a composite image using the layer-staking function of the remote sensing software ERDAS v.14. The raster images obtained were sub-set to the study area using a boundary vector file.

### Landscape classification

**Supervised classification** To classify Landsat pixels into different LULC classes, we used the often-used maximum likelihood supervised classification (MLC) (Lu et al. 2004; Zhang et al. 2016). The MLC is the most common parametric classifier that assumes a normal or near normal spectral distribution for each feature of interest and equal prior probability among the classes. The MLC is based on the probability that a pixel belongs to a particular class. It assumes that these probabilities are the same for all classes, and that the input bands have normal distributions (Li et al. 2011; Lu et al. 2012b).

To specify the various pixel values or spectral signatures that should be associated with each LULC, one hundred and seventy GPS data were randomly selected and used as training samples, and hence the MLC used the spectral signatures from these training areas to classify the whole image (Lu et al. 2005, 2012b; Zhang et al. 2016). Depending on the homogeneity of the LULC type, a polygon of 8–40 pixels for each GPS was selected. Selection of training samples was followed by an evaluation of the spectral separability of the training samples to obtain more accurate values of the training samples where necessary. According to literature, the classification could be reasonably made only if the separability of two training samples is sufficient ( $\geq 10$ ) (Zhang et al. 2016). Finally, the MLC and his function parallelepiped decision rules were applied to the training samples to analyze each pixel and aggregate the pixels into different

LULC types of training samples, and the landscapes were preliminarily classified into different LULC types on a map.

**Post classification** To assess the accuracy of the LULC classifications from Landsat images, the level of error contributed by the LULC image, we used the producer's accuracy, user's accuracy, overall accuracy and kappa coefficient statistics based on a pixel to pixel comparison for the years 2000, 2009 and 2018. The producer's accuracy explains how well a certain LULC type was classified, i.e. how often real features on the ground were correctly shown on the classified map, or the probability that a certain land cover type on the ground was classified as such. The producer's accuracy was computed as the number of reference sites classified accurately divided by the total number of reference sites for that class (Congalton 1991). In contrast, the user's accuracy essentially tells the user how often the class on the map will be present on the ground, which refers to the reliability. This was computed as the fraction of the total number of pixels classified on the total number of correct classifications for a particular LULC for a particular class, and was used to examine the reliability of classified LULC. The overall accuracy often used to assess the performance of each LULC was computed as the fraction of the total number of correctly identified pixels on the total number of pixels (Congalton 1991). The kappa statistics is another accuracy indicator, which measures how the classification results compare to values assigned by chance.

**Analysis to quantify land use and land cover change and trajectories** To quantify the LULC change processes and trajectories in DCF during the two periods, we proceeded with analyses consisting of two stages. First, we conducted a quantification of the area per land cover type for 2000, 2009 and 2018 based on the attribute tables of the land cover maps in ArcGIS 10.5.1. In this way, we could quantify what LULC types increased and what LULC types decreased in land area between 2000–2009 and 2009–2018 and during the whole period 2000–2018. The following parameters were computed for each LULC between 2000–2009, 2009–2018, and the whole period (2000–2018): the absolute change in total area (Ci), the proportional change in area, relative to the initial area (C%), and the annual rate of relative area change (Ar).

This analysis provided the gain or loss for specific LULC types, but did not allow us to quantify the LULC change processes and trajectories or to identify what LULC types had replaced the previous LULC. Therefore, in the second stage, we conducted a change detection at per-pixel using cross-tabulations of the LULC maps, to characterize and analyze the LULC change processes and trajectories, which we call the trajectory analyses. Furthermore, we used the post classification approach to examine the detailed LULC

change trajectories at the per-pixel scale for the three periods following Lu et al. (2013). More specifically, these trajectory analyses consisted of identifying the changes of one Land cover into another land cover and the process implying it (see Appendix S2 for more explanation on land cover change processes and trajectories).

## Results

### Land use/land cover classification and accuracies results

The main aim of this study was to determine the accuracy with which Landsat ETM+ and Landsat OLI can be used to classify the LULC for the three periods. The classification accuracy assessment results for the three periods indicated that the MLC method applied on Landsat images effectively classified the study area into six classes (Fig. 3), providing the fundamental data sources for examining LULC change trajectories.

The computed error matrices for the classified images revealed an overall accuracy of over 80% for the three

classification dates and an overall kappa statistics of over 74% in the classification of the three periods (Table 1). The Classification of LULC using the Landsat 8 OLI for the year 2018 gave the highest classification accuracy (89.45%) and kappa statistics (0.87) compared to the Landsat 7 ETM+ images used for the years 2000 and 2009.

### Status and dynamic of land use and land cover in Doume Communal Forest

The land cover map comparisons showed that in 2000, most of the areas in the DCF were covered with forest (39,520 ha; 98%) and that about 256.94 ha representing 0.65% of this forest area was lost between 2000 and 2009. This percentage represented deforestation of all LULC. Therefore, we observed that during the two decades the forest land cover was facing deforestation and degradation. Hence, dense forest with high tree density (~22,943 ha representing 59% of the total forest) lost about 5% of its area between 2000 and 2009 (Fig. 3, Table 2). This loss continued to increase between 2000 and 2009 (~1099 ha; ~5%) and 2009–2018 (~3864 ha; ~17%). This increased loss corresponded to an annual loss of 0.51 and 1.69, respectively, for 2000–2009

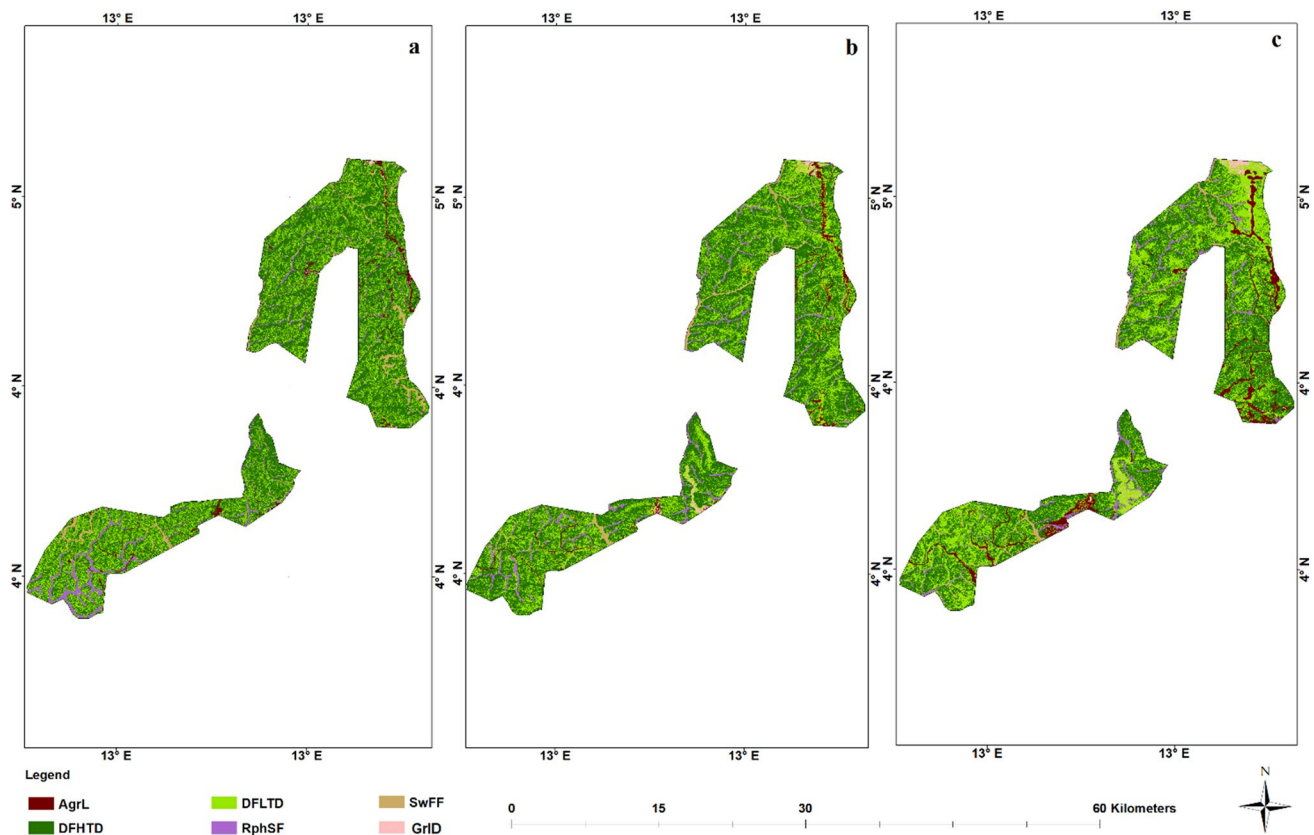


**Fig. 3** Spatio-temporal land use and land cover type of 2000 (a), 2009 (b), and 2018 (c) in the study area (LULC types—AgrL, DFHTD, DFLTD, RphSF, SwFF and GrLD represent agroforestry sys-

tems Land, dense forest with high tree density, dense forest with low tree density, swampy Raphia forest, swampy flooded forest and grasslands, respectively)



**Table 1** Accuracy assessment results for the three periods in the study area

LULC types	AgrL	DFHTD	DFLTD	RphSF	SwFF	GrID	RT	CT	Producers accuracy (%)	Users accuracy (%)
Accuracy assessment for the 2000 classified image										
AgrL	24	0	0	4	0	0	28	26	92.31	85.71
DFHTD	0	15	3	0	2	0	20	17	88.24	75.00
DFLTD	0	1	70	10	7	0	88	90	77.78	79.55
RphSF	2	0	12	48	1	0	63	65	73.85	76.19
SwFF	0	1	4	3	45	0	53	55	81.82	84.91
GrID	0	0	1	0	0	3	4	3	100.00	75.00
Overall classification accuracy = 80.08%; kappa statistics: 0.74										
Accuracy assessment for the 2009 classified image										
AgrL	9	7	0	0	0	2	18	86	95.35	50.00
DFHTD	1	46	3	1	2	2	55	22	77.27	83.64
DFLTD	1	3	17	0	0	0	21	62	88.71	80.95
RphSF	1	1	1	5	0	0	8	61	75.41	62.50
SwFF	4	3	0	2	82	3	94	9	55.56	87.23
GrID	0	1	1	1	2	55	60	16	56.25	91.67
Overall classification accuracy = 83.59%; kappa = 0.78										
Accuracy assessment for the 2018 classified image										
AgrL	3	0	0	0	0	0	3	6	50.00	100.00
DFHTD	0	41	1	0	1	0	43	51	98.15	94.64
DFLTD	1	2	53	0	2	1	59	54	80.39	89.13
RphSF	2	1	0	51	1	0	55	54	94.44	92.73
SwFF	0	5	0	3	61	4	73	66	92.42	83.56
GrID	0	2	0	0	1	20	23	25	80.00	86.96
Overall classification accuracy = 89.45%; kappa statistics = 0.87										

LULC types—AgrL, DFHTD, DFLTD, RphSF, SwFF and GrID represent agroforestry systems land, dense forest with high tree density, dense forest with low tree density, swampy Raphia forest, swampy flooded forest and grassland, respectively. RT and CT represent row total and column total, respectively

**Table 2** Change in land use and land cover from 2000 to 2009 in Doume Communal Forest in eastern Cameroon

LULC type	2000		2009		LULC change between 2000 and 2009			
	Area (ha)	%	Area (ha)	%	Area (ha)	%	Annual change rate (ha)	%
AgrL	882.54	2.18	1139.48	2.82	256.94	29.11	28.55	3.23
DFHTD	23,943.03	59.26	22,843.50	56.54	−1099.54	−4.59	−122.17	−0.51
DFLTD	12,239.92	30.30	13,308.69	32.94	1068.76	8.73	118.75	0.97
RphSF	2010.26	4.98	1934.33	4.79	−75.93	−3.78	−8.44	−0.42
SwFF	1170.93	2.90	900.95	2.23	−269.98	−23.06	−30.00	−2.56
GrID	155.37	0.38	275.55	0.68	120.18	77.35	13.35	8.59
Total	40,402.50	100	40,402.50	100	—	—	—	—

LULC types—AgrL, DFHTD, DFLTD, RphSF, SwFF and GrID represent agroforestry systems Land, dense forest with high tree density, dense forest with low tree density, swampy Raphia forest, swampy flooded forest and grassland, respectively

and 2009–2018 (Tables 2, 3). Not only the dense forest with high trees density surfaces decreased, but also the swampy Raphia and swampy flooded forests in terms of canopy cover. Swampy Raphia forest declined from 2000–2009 by ~4% to ~11% in 2009–2018 while Swampy flooded forests

declined from 2000–2009 by 270 ha (~23%) to 295 (~25%) (Fig. 3, Tables 2, 3). In contrast, at the same time, significant improvements in other LULC (e.g. agricultural areas, grassland areas and dense forest with low trees density areas) were observed. Dense forest with low tree density

**Table 3** Change in land use and land cover from 2009 to 2018 in Doume Communal Forest in eastern Cameroon

LULC type	2009		2018		LULC change between 2009 and 2018			
	Area (ha)	%	Area (ha)	%	Area (ha)	%	Annual change rate (ha)	%
AgrL	1139.48	2.82	2561.10	6.34	1421.62	124.76	142.16	12.48
DFHTD	22,843.50	56.54	18,979.44	46.98	− 3864.06	− 16.92	− 386.41	− 1.69
DFLTD	13,308.69	32.94	15,799.00	39.10	2490.31	18.71	249.03	1.87
RphSF	1934.33	4.79	1731.31	4.29	− 203.02	− 10.50	− 20.30	− 1.05
SwFF	900.95	2.23	875.88	2.17	− 25.07	− 2.78	− 2.51	− 0.28
GrID	275.55	0.68	455.77	1.13	180.22	65.40	18.02	6.54
Total	40,402.50	100.00	40,402.50	100.00	–	–	–	–

LULC types—AgrL, DFHTD, DFLTD, RphSF, SwFF and GrID represent agroforestry systems land, dense forest with high tree density, dense forest with low tree density, swampy Raphia forest, swampy flooded forest and grassland, respectively

increased between 2000–2009 and 2009–2018 in terms of land area from 1069 ha (9%) to 2490 ha (19%), respectively (Fig. 3, Tables 2, 3). It was observed that the area of agroforestry systems had almost tripled from 882 ha in 2000 to almost 2561 ha in 2018 (Table 4). This expansion of agroforestry systems was observed to be at an annual rate of 10% during the two decades. Grassland also increased from 120 ha (78%) up to 180 ha (65%) between 2000–2009 and 2009–2018. The changes occurred in the dense forest with high tree density areas over time are a direct effect of the changes in agroforestry systems land, dense forest with low density and grassland in 19 years (Table 4).

### Change trajectories of land use and land cover in Doume Communal Forest

The main LULC change processes and trajectories in the period 2000–2018, as identified after post-classification (thick arrows in Fig. S1 show the dominant processes) were large-scale degradation, deforestation and subsequently conversions of forest land. On a less common

basis, restoration occurred from dense vegetation with low tree density to dense vegetation with high tree density. Furthermore, the abandonment and regeneration of forest from agroforestry systems to the dense forest were recorded.

In this study, the same trajectories were identified during the first, the second and the entire period of the study. The following trajectories were identified in order of complexity:

- multiple-step trajectories of (1) forest degradation, (2) deforestation and (3) conversion of dense forest to agroforestry systems land; (4) the passage of dense forest with high tree density into swampy flooded forest under specific climatic conditions;
- multiple-step trajectories of (1) degradation, (2) restoration of dense forest with low tree density to high tree density, (3) conversion of dense forest to agroforestry systems, and (4) abandonment and regeneration; (5) the passage of dense forest with low tree density into swampy flooded forest under specific climatic conditions;

**Table 4** Change in land use and land cover in the last two decades in Doume Communal Forest in eastern Cameroon

LULC type	2000		2018		LULC Change between 2000 and 2018			
	Area (ha)	%	Area (ha)	%	Area (ha)	%	Annual change rate (ha)	%
AgrL	882.54	2.18	2561.10	6.34	1678.56	190.20	88.35	10.01
DFHTD	23,943.03	59.26	18,979.44	46.98	− 4963.59	− 20.73	− 275.76	− 1.09
DFLTD	12,239.92	30.30	15,799.00	39.10	3559.08	29.08	187.32	1.53
RphSF	2010.26	4.98	1731.31	4.29	− 278.94	− 13.88	− 14.68	− 0.73
SwFF	1170.93	2.90	875.88	2.17	− 295.05	− 25.20	− 15.53	− 1.33
GrID	155.37	0.38	455.77	1.13	300.40	193.35	15.81	10.18
Total	40,402.50	100	40,402.50	100	–	–	–	–

LULC types—AgrL, DFHTD, DFLTD, RphSF, SwFF and GrID represent agroforestry systems land, dense forest with high trees density, dense forest with low tree density, swampy Raphia forest, swampy flooded forest and grassland, respectively

- multiple-step trajectories of (1) conversion of forest to agroforestry systems land and (2) abandonment and regeneration;
- multiple-step trajectories of (1) degradation, and (2) abandonment and regeneration;
- two-step trajectories of (1) conversion of grassland to agroforestry systems land, and (2) abandonment and regeneration.

### Quantification and schematic presentation of land use and land cover change processes and trajectories

From the pixel-to-pixel cross tabulations (Table S4–Table S9), we were able to quantify and characterize the specific land cover change processes and trajectories that had occurred in the DCF and which resulted in forest change (see Fig. 4a, b, Table 5). Between 2000 and 2018, about 53.45% (~21,583 ha) of the LULC in the study area had changed (Table 5). Figure 4a, b and Table 5 show that in the periods 2000–2009 and 2009–2018, most of the loss of dense forest with high tree density to a dense forest with low tree density and swampy Raphia was caused by degradation,

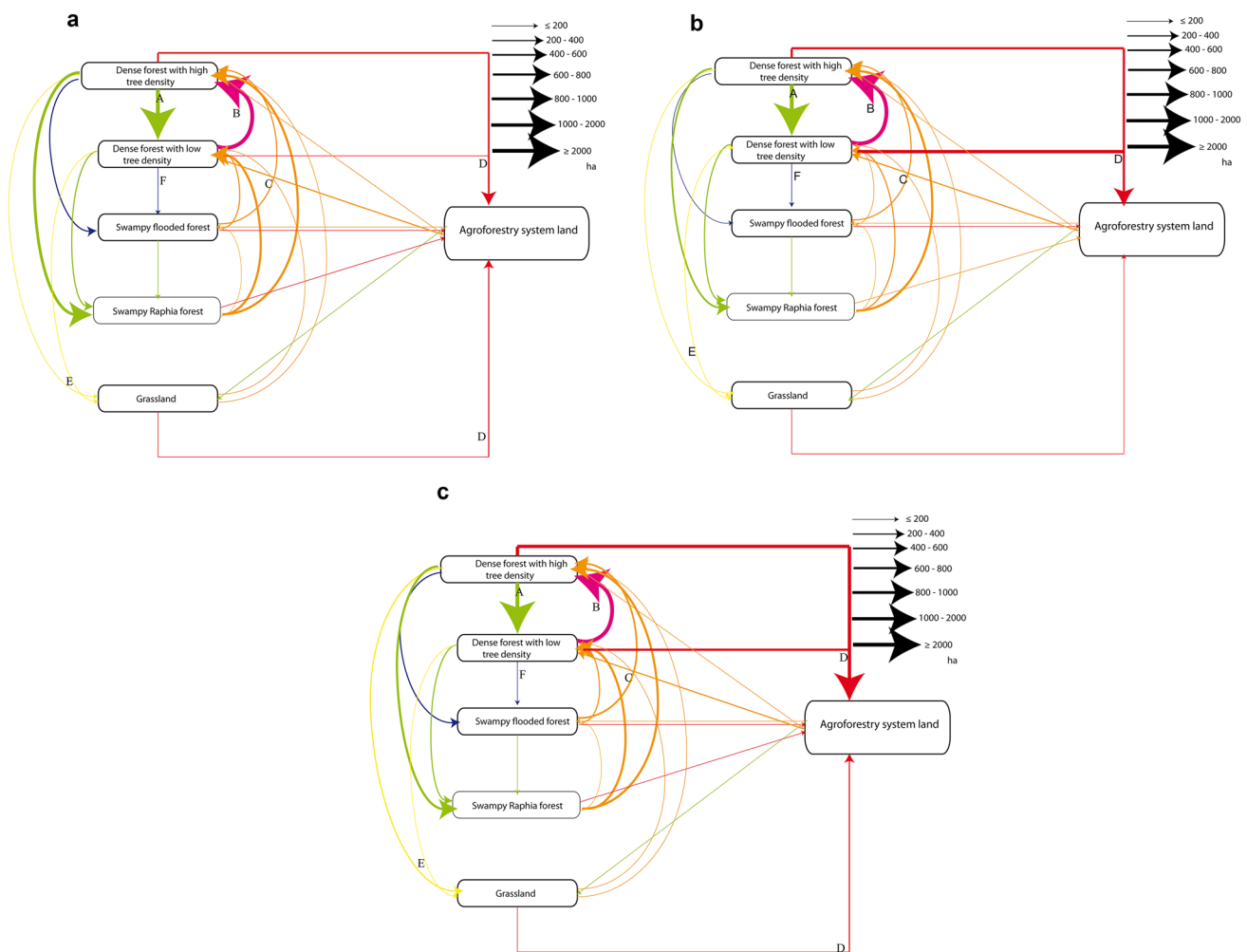


**Fig. 4** Quantification and schematic presentation of the LULC change processes and trajectories in the Doume communal Forest based on the pixel-to-pixel cross-tabulations of the land cover maps. Each arrow shows the change from one land use and land cover type to another that occurred from 2000–2009 (a), from 2009–2018 (b) and 2000–2018 (c). The thickness and the color of each arrow indicate the area of change for each of the trajectories and the processes within the given period, respectively. The trajectories are either dominant

(thick of arrows) or less dominant (thin arrows): (A: green) degradation to dense forest with low tree density or swampy Raphia forest; (B: pink) restoration of degraded dense forest with low tree density into dense forest with high tree density; (C: orange) abandonment and regeneration; (D: red) conversion of forest and grassland into agroforestry systems; (E: yellow) deforestation to grassland; (F: blue) the passage of dense forests into swampy flooded forest which occurred under specific climatic conditions

**Table 5** Quantified land use and land cover change processes based on remote sensing data that occurred in the periods 2000–2009, 2000–2009 and 2000–2018

Land cover process	Area (ha)			Area (%)			Annual change rate (%)		
	2000–2009	2009–2018	2000–2018	2000–2009	2009–2018	2000–2018			
Deforestation	1377	1191	1481	6.76	6.84	6.86	0.68	0.76	0.38
Degradation	7904	7757	9240	38.81	44.54	42.81	3.88	4.95	2.38
Conversion	734	1916	2164	3.60	11.00	10.02	0.36	1.20	0.55
Restoration	7372	4283	5645	36.20	24.59	26.15	3.62	2.73	1.45
Abandonment, and regeneration	2491	1976	2820	12.23	11.35	13.07	1.22	1.26	0.72
Species colonisation and climatic conditions	488	293	233	2.40	1.68	1.08	0.24	0.19	0.06
Total land change	20,366	17,416	21,583						
No change land	20,016	22,966	18,799						
TOTAL	40,382	40,382	40,382	100.00	100.00	100.00			

direct conversions to agroforestry systems and the dense forest by deforestation to grassland. In more details, over the 19 years analyzed, degradation entailed 9240 ha or 43% of the total land cover change, conversions from forest to agroforestry systems entailed 2164 ha or 10%, and deforestation of dense forest to grassland entailed 1481 ha or 7% of the total land cover change (Table 5). Table S4–Table S9, show the hectares and percentage of the area. For example, from 2000 to 2009, almost 8601 ha of dense forest with high tree density was degraded to a dense forest with low tree density, while about 1128 ha was converted into agroforestry systems and 153 ha was deforested to grassland. Furthermore, in the period 2009–2018, an additional 7646 ha of dense forest with high tree density was degraded to low tree density and swampy *Raphia* forest, and 1191 ha were deforested to grassland. In contrast, in that same period (2009–2018), 2164 ha of forest and grassland was converted and afforested respectively into agroforestry systems.

Between 2000 and 2018, about 99% of the total area of land cover change had changed through multiple-step trajectories (see the arrows in Fig. 4c), meaning that land cover had changed from one type to several other land cover types within the total study period. Only ~1% of the total area of land cover change had changed through two-step trajectories between 2000 and 2018, indicating that land cover had changed from one type to a second type and further to a third type. The first type of multiple-step trajectories that had occurred in the landscape (in terms of land area, namely ~11,743 ha in total) involved forest degradation (from more dense forest with high tree density to more dense forest with low tree density types and swampy *Raphia* forest), deforestation (from dense forest with high tree density to grassland) and conversion (from dense forest with high tree density to agroforestry systems). The second type of multiple-step trajectories involved changes from the dense forest with low tree density (6983 ha in total) to a dense forest with high

tree density (i.e., restoration), to swampy *Raphia* forest (i.e. degradation) or grassland (i.e., deforestation), and further to agroforestry systems (i.e., conversions). The third type of multiple-steps, trajectories involved changes from swampy *Raphia* forest (2008 ha in total) to agroforestry systems (i.e. conversions), and to dense forest (i.e. abandonment and regeneration); the fourth type of multiple steps trajectories involved degradation of agroforestry systems (882 ha in total) into grassland, and abandonment and regeneration (dense forest, and swampy flood forest); and the last multiple steps trajectories involved conversion of grassland (161 ha) into agroforestry systems land, and abandonment and regeneration (dense forest).

The increase in the number of arrows in Fig. 3b compared to Fig. 3a clearly shows that the area and the different types of land cover increased but kept the same set of trajectories in the period 2009–2018, compared to 2000–2009. Deforestation to grassland decreased between 2000 and 2018 and entailed a total land area of ~1377 ha in 2000–2009 and ~1191 ha in 2009–2018, which is about 6.76% and 6.84% of the total land cover change area in these periods, respectively.

Moreover, degradation decreased from ~7904 ha or 38.81% of the total land cover in the period 2000–2009 to ~7757 ha or 44.54% in 2009–2018. Conversion from forest to agroforestry systems increased from ~734 ha or 3.60% in 2000–2009 to ~1916 ha or 11% between these two periods. Other types of land cover change processes can be found in Table 5.

## Discussion

We first evaluated how accurately the Landsat images classified the study area into different thematic areas. For the three periods, both images effectively classify the study area into



six thematic maps. We then assess the dynamic change and change trajectories of LULC during two decades.

### Landscape classification

The LULC types in the study area were interpreted on imagery by MLC supervised classification. With the overall accuracies and kappa statistics of the three periods LULC classification scheme all above 80% and 0.74, respectively, substantiating the ability of Landsat products to accurately classify tropical dense rainforest of Cameroon. However, 80 and 83% accuracy of the 2000 and 2009 land cover maps, respectively, are acceptable but point towards a sub-optimal LULC classification, which may lead to a wrong interpretation of the timing of changes or even wrong trajectories. Moreover, the lack of a clear boundary between LULC in our forest was due to the complex vegetation structure and species composition causing a major problem of relatively low accuracy for the two first-year periods: justifying thereby the misclassification between LULC (e.g. agroforestry systems land use types such as cocoa-based agroforestry systems, banana plantations and dense forest with high tree density, dense forest with low tree density, swampy *Raphia* forest, swamp floods forest and wooded savanna LULC types). These findings are in line with the findings of Lu et al. (2013) in Amazonia forests and of Zhang et al. (2016) in the forest of China. However, the high accuracy (89.45%) of LULC classification obtained for the 2018 year, using Landsat 8 OLI allow us to conclude that high-resolution satellite imagery is consequential to high ability LULC classification scheme, therefore, highlighting the unavoidable availability of high-resolution satellite images for efficiently monitoring, sustainable management of Congo Basin forests.

### Dynamic and change trajectories of land use and land cover in Doume Communal Forest

Information on detailed LULC change trajectories is often required for spatio-temporal dynamics research and is often calculated using the post-classification method at the per-pixel level as reported by several authors worldwide (Lambin 2000; Kennedy et al. 2009; Hansen and Loveland 2012; Lu et al. 2014). First of all, the post-classification method at the overall scale, allows us to analyze the status and overall forest cover changes whereby the loss and gain of LULC in the DCF was realized. This study showed that the DCF is experiencing an essentially regressive evolution which was much more significant in dense forest with high tree density LULC. Indeed, from 2000 to 2009 this LULC loss approximately 5% of its areas in benefits principally to agroforestry systems and dense forest with low tree density LULC types which gained 29 and 9% of their areas during the same periods, respectively. Several authors across Cameroon and

Africa have reported a similar trend (Momo Solefack et al. 2012; De Wasseige et al. 2014; Meli Fokeng and Meli Meli 2015; Momo Solefack et al. 2018; Temgoua et al. 2018; Toh et al. 2018).

The overall-scale change detection results cannot provide the change trajectories, but the per-pixel based change detection analysis overcomes this shortcoming. Therefore, in this study, we have integrated pixel-to-pixel cross-tabulations of LULC change and our knowledge to generate a more comprehensive analysis of the main LULC change processes and trajectories in the DCF. Our findings show that most of the land cover changes between 2000 and 2018 involved degradation (~43% of total land cover change), restoration from dense forest with low trees density to those of high trees density (26%), conversion from forest to agroforestry systems (10%) and deforestation to Swampy *Raphia* forest and grassland (~7%). This high presence of forest degradation and conversion from forest to agroforestry systems may partly be related to the extensive and recurring population in the communal forest who practice agroforestry for their subsistence. Furthermore, the combined analyses showed that from 2000–2009 to 2009–2018 periods, a decreasing shift occurred in the main processes of forest degradation, deforestation but an increasing shift occurred from forest to agroforestry systems. This study points out that agroforestry systems but not land use types of agroforestry systems are the main drivers of deforestation and conversion in the DCF. These findings are in line with the findings of Lu et al. (2013) in the Brazilian Amazon forest. This shift does not coincide totally with the process of forest classification into a communal forest: before 2000, the DCF was facing anthropogenic pressures and illegal logging, while after 2009, access to DFC was strictly prohibited to riparian population and that its management was subject to a well-planned management. Therefore, we expected that we could have had regression of deforestation and conversion from forest to agroforestry systems during the second period of the study. This finding highlights the anthropogenic influence on forests even though access was strictly prohibited, thus dismissing the question on the distribution of the benefits resulting from the management of the forest. The DFC is not the only communal forest in Cameroon facing this phenomenon because it has also been reported in Santchou Reserve by Meli Fokeng and Meli Meli (2015), in Koupa-Matapit Gallery Forest by Momo Solefack et al. (2018), and in Mount Bamboutos Caldera by Toh et al. (2018).

### Implications for sustainable management and conservation of forest

Our study shows that analyses of landscape trajectories can provide a more comprehensive overview on which land cover types are involved in other land cover change and

forest regressions and how this land cover interacts with one another. This is particularly important for spatial planning in tropical forests where agriculture develops rapidly (Lambin 1997, 2000; Lu et al. 2013). Conversions into agroforestry systems can be identified and monitored by such trajectory analyses, and subsequently, zoning conservation and management policies can be developed to guide these changes into more sustainable directions. This is particularly important since such changes can change the socio-cultural environment of the ecosystem, impact on the production of ecosystem services and, therefore, result in a loss of biodiversity and carbon pools. Therefore, it is essential and recommended that communities should be involved in the spatial planning and management process as they may play an important role in LULC change and may be affected by it. To reduce the pressures of the riparian population into the DFC, the managers could put in place some incentivized methods, for example by REDD+ or through subsidies for local food production.

## Conclusions

Through the analysis of LULC change based on three dates of Landsat imagery in the Doume Communal Forest, this research highlights the necessity to investigate LULC change at multiple scales for a better understanding of the mechanisms of LULC change and the effective use of the LULC results in multidisciplinary research. Therefore, this study enables us to identify the spatial patterns and LULC change trajectories. It also suggests the mechanisms related to LULC in DFC. It highlights the necessity for the availability of high-resolution satellite images for efficiently monitoring and sustainable management of Congo Basin forests. This study showed a LULC change of about one-half of the study area in the period 2000–2009. Based on our quantitative and spatial analyses, forest degradation, restoration, conversion of forest and grassland to agroforestry systems and deforestation to swampy *Raphia* forest and grassland were found to be the dominant LULC change processes causing reduction of forest cover and quality. In addition, the post-classification based on per pixel scale showed that the different types of LULC changes in the study area increased and involved a more diverse set of characteristic trajectories in the period 2009–2018, compared to the period 2000–2009. During 2000 and 2018, about 99% of the total area of LULC changed through multiple-step trajectories and 1% by one-step trajectories, and most trajectories involved deforestation, degradation, conversion of forest and grassland to agroforestry systems land, and abandonment, regrowth and recolonization of the environment. Deforestation to grassland decreased between 2000 and 2018 and entailed a total land area of ~1377 ha in 2000–2009 and ~1191 ha in

2009–2018 which is about 6.76 and 6.84%, respectively, of the total land cover change area in these periods. However, degradation increased from 38.8% of the total LULC change in the period 2000–2009 to 44.54% in 2009–2018. Conversion from the forest and grassland to agroforestry systems increased from 3.60% in 2000–2009 to 11% in 2009–2018. The trajectory analyses showed that LULC change occurred mostly in multiple-step trajectories of degradation, deforestation and conversion; multiple step trajectories from the dense forest with high tree density to a dense forest with low tree density, grassland, swampy *Raphia* forest and further to agroforestry systems. Therefore, the trajectory analysis of this study showed important interlinkages between LULC. It is a necessity to further understand and account for such interlinkages and processes of change to guide management in more sustainable ways.

**Acknowledgements** The lead author is grateful for the PhD exchange scholarship given by the Transdisciplinary Training for Resource Efficiency and Climate Change Adaptation in Africa (TRECCAfrica II) project funded by the European Union. The research leading to these results has received financial funding from the British Ecological Society (EA17/1005) and The Rufford Foundation (Grant agreement N° 24,895-1), and field material funding from the IDEA WILD Foundation. We thank Dr Masha T. van der Sande for their comments and suggestions on the first manuscript of this paper. We are grateful to the Conservation and Sustainable Natural Resources Management Network (CSNRM-Net) Association for their logistical and technical support during the entire study. The authors would like to thank the National Aeronautics and Space Administration (NASA), United States Geological Survey (USGS) for providing Landsat data. We would also thank Airbus Defense and Space through the project “Observation Spatiale des Forêts d’Afrique Centrale et de l’Ouest” (OSFACO) for providing SPOT 7 images. We are also grateful to Doume municipality for their logistical support during the fieldwork. Specifically, we thank the mayoreess of the Doume municipality Mrs Mpans Giselle Rose and her secretary Mrs Ayinda Yannick for their administrative diligence and for providing us with field permits. We, furthermore, express our thanks to all those involved in fieldwork and data collection as well as community members of the different village of Doume council.

## Compliance with ethical standards

**Conflict of interest** The authors declare no conflict of interest.

## References

- Anonymous (2015) Management plan of the Doume Communal Forest. Doume Council, Yaounde Cameroon
- Basnet B, Vodacek A (2015) Tracking land use/land cover dynamics in cloud prone areas using moderate resolution satellite data: a case study in Central Africa remote sensing 7:6683
- Bellard C, Bertelsmeier C, Leadley P, Thuiller W, Courchamp F (2012) Impacts of climate change on the future of biodiversity. *Ecol Lett* 15:365–377. <https://doi.org/10.1111/j.1461-0248.2011.01736.x>
- CBD (2005) Handbook of the convention on biological diversity including its Cartagena protocol on biosafety, 3rd edn. Secretariat of the Convention on Biological Diversity, United Nations, Montreal

- Chitade AZ, Katiyar SK (2012) Multiresolution and multispectral data fusion using discrete wavelet transform with IRS images: Cartosat-1, IRS LISS III and LISS IV. *J Indian Soc Remote Sens* 40:121–128. <https://doi.org/10.1007/s12524-011-0140-0>
- Congalton RG (1991) A review of assessing the accuracy of classifications of remotely sensed data. *Remote Sens Environ* 37:35–46. [https://doi.org/10.1016/0034-4257\(91\)90048-B](https://doi.org/10.1016/0034-4257(91)90048-B)
- Davies-Barnard T, Valdes PJ, Singarayer JS, Wiltshire AJ, Jones CD (2015) Quantifying the relative importance of land cover change from climate and land use in the representative concentration pathways. *Glob Biogeochem Cycles* 29:842–853. <https://doi.org/10.1002/2014GB004949>
- De Wasseige C, Devers D, Marcken P, Eba'a Atyi R, Nasi R, Mayaux P (2009) The forests of the Congo Basin—state of the forest 2008. Office des publications de l'Union Européenne, Brussels
- De Wasseige C, Flynn J, Louppe D, Hiol Hiol F, Mayaux P (2014) The forests of the Congo Basin—state of the forest 2013. Weyrich, Neufchâteau
- Dimiyati MUH, Mizuno KEI, Kobayashi S, Kitamura T (1996) An analysis of land use/cover change in Indonesia. *Int J Remote Sens* 17:931–944. <https://doi.org/10.1080/01431169608949056>
- Ehlers M (2004) Spectral characteristics preserving image fusion based on Fourier domain filtering. In: *Remote Sensing for Environmental Monitoring, GIS Applications, and Geology IV*, Maspalomas, Canary Islands, Spain, 2004. Society of Photo-Optical Instrumentation Engineers (SPIE), p 13. <https://doi.org/10.1117/12.565160>
- Ellis EC, Goldewijk KK, Siebert S, Lightman D, Ramankutty N (2010) Anthropogenic transformation of the biomes, 1700 to 2000. *Glob Ecol Biogeogr* 19:589–606. <https://doi.org/10.1111/j.1466-8238.2010.00540.x>
- FAO (2006) Global forest resources assessment 2005: progress towards sustainable forest management Rome. United Nations Food and Agriculture Organization, Rome
- FAO (2011) State of the world's forests. Food and Agriculture Organization of United Nations (FAO), Rome
- Foley JA et al (2005) Global consequences of land use *Science* 309:570–574. <https://doi.org/10.1126/science.1111772>
- Geist HJ, Lambin EF (2002) Proximate causes and underlying driving forces of tropical deforestation. *BioScience* 52:143. [https://doi.org/10.1641/0006-3568\(2002\)052%5b0143:pcaudf%5d2.0.co;2](https://doi.org/10.1641/0006-3568(2002)052%5b0143:pcaudf%5d2.0.co;2)
- Ghilardi A et al (2016) Spatiotemporal modeling of fuelwood environmental impacts: towards improved accounting for non-renewable biomass. *Environ Model Softw* 82:241–254. <https://doi.org/10.1016/j.envsoft.2016.04.023>
- Gibbs HK, Ruesch AS, Achard F, Clayton MK, Holmgren P, Ramanakutty N, Foley JA (2010) Tropical forests were the primary sources of new agricultural land in the 1980s and 1990s. *Proc Natl Acad Sci USA* 107:16732–16737. <https://doi.org/10.1073/pnas.0910275107>
- Gidey E, Dikinya O, Sebego R, Segosebe E, Zenebe A (2017) Modeling the spatio-temporal dynamics and evolution of land use and land cover (1984–2015) using remote sensing and GIS in Raya, Northern Ethiopia. *Model Earth Syst Environ* 3:1285–1301. <https://doi.org/10.1007/s40808-017-0375-z>
- Grainger A (2008) Difficulties in tracking the long-term global trend in tropical forest area. *Proc Natl Acad Sci USA* 105:818–823. <https://doi.org/10.1073/pnas.0703015105>
- Grainger A (2010) Uncertainty in the construction of global knowledge of tropical forests. *Prog Phys Geogr Earth Environ* 34:811–844. <https://doi.org/10.1177/0309133310387326>
- Hansen MC, Loveland TR (2012) A review of large area monitoring of land cover change using Landsat data. *Remote Sens Environ* 122:66–74. <https://doi.org/10.1016/j.rse.2011.08.024>
- Harris NL et al (2012) Baseline map of carbon emissions from deforestation in tropical regions. *Science* 336:1573–1576. <https://doi.org/10.1126/science.1217962>
- Kennedy RE, Townsend PA, Gross JE, Cohen WB, Bolstad P, Wang YQ, Adams P (2009) Remote sensing change detection tools for natural resource managers: understanding concepts and tradeoffs in the design of landscape monitoring projects. *Remote Sens Environ* 113:1382–1396. <https://doi.org/10.1016/j.rse.2008.07.018>
- Kibret KS, Marohn C, Cadisch G (2016) Assessment of land use and land cover change in South Central Ethiopia during four decades based on integrated analysis of multi-temporal images and geospatial vector data. *Remote Sens Appl Soc Environ* 3:1–19. <https://doi.org/10.1016/j.rsase.2015.11.005>
- Kindu M, Schneider T, Döllner M, Teketay D, Knoke T (2018) Scenario modelling of land use/land cover changes in Munessa–Shashemene landscape of the Ethiopian highlands. *Sci Total Environ* 622–623:534–546. <https://doi.org/10.1016/j.scitotenv.2017.11.338>
- Lambin EF (1997) Modelling and monitoring land-cover change processes in tropical regions. *Prog Phys Geogr Earth Environ* 21:375–393. <https://doi.org/10.1177/030913339702100303>
- Lambin EF (2000) Land-cover-change trajectories in southern Cameroon. *AU Mertens Benoît Ann Assoc Am Geogr* 90:467–494. <https://doi.org/10.1111/0004-5608.00205>
- Lambin EF et al (2001) The causes of land-use and land-cover change: moving beyond the myths. *Glob Environ Change* 11:261–269. [https://doi.org/10.1016/S0959-3780\(01\)00007-3](https://doi.org/10.1016/S0959-3780(01)00007-3)
- Le Quéré C et al (2013) The global carbon budget 1959–2011. *Earth Syst Sci Data* 5:165–185. <https://doi.org/10.5194/essd-5-165-2013>
- Le Quéré C et al (2016) Global carbon budget 2016. *Earth Syst Sci Data* 8:605–649. <https://doi.org/10.5194/essd-8-605-2016>
- Le Toan T, Quegan S, Davidson M et al (2011) The biomass mission: mapping global forest biomass to better understand the terrestrial carbon cycle. *Remote Sens Environ* 115:2850–2860
- Letouzey R (1985) Phytogeographic map of Cameroon at 1: 500 000, accompanied by: Notice of the phytogeographic map of Cameroon at 1: 500 000. 4) TV: Domain of dense rainforest always green (Pages 95 to 142 with groupings n° 185 to 267). Institute of the International Vegetation Map, Toulouse
- Lewis SL et al (2009) Increasing carbon storage in intact African tropical forests. *Nature* 457:1003–1006
- Li G, Lu D, Moran E, Hetrick S (2011) Land-cover classification in a moist tropical region of Brazil with Landsat TM imagery. *Int J Remote Sens* 32:8207–8230. <https://doi.org/10.1080/01431161.2010.532831>
- Lu D, Mauseel P, Brondizio E, Moran E (2004) Change detection techniques. *Int J Remote Sens* 25:2365–2401. <https://doi.org/10.1080/0143116031000139863>
- Lu D, Batistella M, Moran E, De Miranda E (2005) A comparative study of terra ASTER, landsat TM, and SPOT HRG data for land cover classification in the Brazilian Amazon. In: *WMSCI 2005—the 9th world multi-conference on systemics, cybernetics and informatics, proceedings, Orlando, Florida, USA, 10–13 Jul 2005*, pp 411–416
- Lu D, Li G, Moran E, Dutra L, Batistella M (2011) A comparison of multisensor integration methods for land cover classification in the Brazilian Amazon. *GISci Remote Sens* 48:345–370. <https://doi.org/10.2747/1548-1603.48.3.345>
- Lu D, Hetrick S, Moran E, Li G (2012a) Application of time series landsat images to examining land-use/land-cover dynamic change. *Photogramm Eng Remote Sens* 78:747–755. <https://doi.org/10.14358/PERS.78.7.747>
- Lu D, Batistella M, Li G, Moran E, Hetrick S, Freitas CdC, Dutra LV, Sant'Anna SJS (2012b) Land use/cover classification in the Brazilian Amazon using satellite images. *Pesq Agropec Bras* 47:1185–1208. <https://doi.org/10.1590/S0100-204x2012000900004>
- Lu D, Li G, Moran E, Hetrick S (2013) Spatiotemporal analysis of land use and land cover change in the Brazilian Amazon. *Int J*

- Remote Sens 34:5953–5978. <https://doi.org/10.1080/01431161.2013.802825>
- Lu D, Li G, Moran E (2014) Current situation and needs of change detection techniques. *Int J Image Data Fusion* 5:13–38. <https://doi.org/10.1080/19479832.2013.868372>
- Malhi Y, Gardner TA, Goldsmith GR, Silman MR, Zelazowski P (2014) Tropical forests in the anthropocene. *Annu Rev Environ Resour* 39:125–159. <https://doi.org/10.1146/annurev-envir-030713-155141>
- Marchese C (2015) Biodiversity hotspots: a shortcut for a more complicated concept. *Glob Ecol Conserv* 3:297–309. <https://doi.org/10.1016/j.gecco.2014.12.008>
- Meli Fokeng R, Meli Meli V (2015) Modeling drivers of forest cover change in the Santchou wildlife reserve, west Cameroon using remote sensing and land use dynamics degree indexes. *Can J Trop Geogr* 2:29–42
- Miheretu BA, Yimer AA (2017) Land use/land cover changes and their environmental implications in the Gelana sub-watershed of Northern highlands of Ethiopia. *Environ Syst Res* 6:7. <https://doi.org/10.1186/s40068-017-0084-7>
- Momo Solefack MC, Chaberrie O, Gallet-Moron E, Nkongmeneck B-A, Leumbe ONL, Decocq G (2012) Analysing deforestation by remote sensing coupled with structural equation models: example of the cloud forest of mount Oku (Cameroon). *Acta Bot Gallica* 159:451–466. <https://doi.org/10.1080/12538078.2012.750583>
- Momo Solefack MC, Njouonkouo AL, Temgoua LF, Djouda Zangmene R, Wouokoue Taffo JB, Ntoupka M (2018) Land use/land cover change and anthropogenic causes around Koupa-Matapit gallery forest, West-Cameroon. *J Geogr Geol* 10:56
- Myers N (1988) Threatened biotas: “Hot spots” in tropical forests. *Environmentalist* 8:187–208. <https://doi.org/10.1007/bf02240252>
- Pendrill F, Persson UM (2017) Combining global land cover datasets to quantify agricultural expansion into forests in Latin America: limitations and challenges. *PLoS One* 12:e0181202. <https://doi.org/10.1371/journal.pone.0181202>
- Pradhan B, Lee S, Mansor S, Buchroithner M, Jamaluddin N, Khujaimah Z (2008) Utilization of optical remote sensing data and geographic information system tools for regional landslide hazard analysis by using binomial logistic regression model. *J Appl Remote Sens* 2(1):1–11. <https://doi.org/10.1117/1.3026536>
- Ramankutty N, Gibbs HK, Achard F, Defries R, Foley JA, Houghton RA (2007) Challenges to estimating carbon emissions from tropical deforestation. *Glob Change Biol* 13:51–66. <https://doi.org/10.1111/j.1365-2486.2006.01272.x>
- Rawat JS, Kumar M (2015) Monitoring land use/cover change using remote sensing and GIS techniques: a case study of Hawalbagh block, district Almora, Uttarakhand, India. *Egypt J Remote Sens Space Sci* 18:77–84. <https://doi.org/10.1016/j.ejrs.2015.02.002>
- Sangermano F, Toledano J, Eastman JR (2012) Land cover change in the Bolivian Amazon and its implications for REDD+ and endemic biodiversity. *Landsc Ecol* 27:571–584. <https://doi.org/10.1007/s10980-012-9710-y>
- Sebastian O, Sibyll S, Wolfgang L, Dieter G (2015) Three centuries of dual pressure from land use and climate change on the biosphere. *Environ Res Lett* 10:044011
- Singh SK, Laari PB, Mustak S, Srivastava PK, Szabó S (2017) Modeling of land use land cover change using earth observation datasets of Tons River Basin, Madhya Pradesh, India. *Geocarto Int*. <https://doi.org/10.1080/10106049.2017.1343390>
- Smail RA, Lewis DJ (2009) Forest-land conversion, ecosystem services, and economic issues for policy: a review. U.S. Department of Agriculture, Forest Service, Pacific Northwest Research Station, Corvallis
- Temgoua LF, Momo Solefack MC, Nguimdo Voufo V, Tagne Belibi C, Tanougong A (2018) Spatial and temporal dynamic of land-cover/land-use and carbon stocks in Eastern Cameroon: a case study of the teaching and research forest of the University of Dschang. *For Sci Technol* 14:181–191. <https://doi.org/10.1080/21580103.2018.1520743>
- Toh FA, Angwafo T, Ndam LM, Antoine MZ (2018) The socio-economic impact of land use and land cover change on the inhabitants of Mount Bambouto Caldera of the Western Highlands of Cameroon. *Adv Remote Sens* 7:25–45. <https://doi.org/10.4236/ars.2018.71003>
- World Resources Institute UNEP, United Nations Development Programme & World Bank (1998) *World Resources 1998–99*. Oxford University Press, New York
- Wu M, Schurgers G, Ahlström A, Rummukainen M, Miller PA, Smith B, May W (2017) Impacts of land use on climate and ecosystem productivity over the Amazon and the South American continent. *Environ Res Lett* 12:054016
- Zari MP (2014) Ecosystem services analysis in response to biodiversity loss caused by the built environment. *Surv Perspect Integr Environ Soc* 7:1–14
- Zhang Z, Zang R, Wang G, Huang X (2016) Classification of landscape types based on land cover, successional stages and plant functional groups in a species-rich forest in Hainan Island, China. *Trop Conserv Sci* 9:135–152. <https://doi.org/10.1177/194008291600900107>

**Publisher's Note** Springer Nature remains neutral with regard to jurisdictional claims in published maps and institutional affiliations.